Available online at www.sciencedirect.com
SCIENCE DIRECT
ELSEVIER
Polymer 46 (2005) 7612–7623
polymer
www.elsevier.com/locate/polymer

Organically modified layered-silicates facilitate the formation of interconnected structure in the reaction-induced phase separation of epoxy/thermoplastic hybrid nanocomposite

Mao Peng[a,*], Hongbing Li[b], Lijuan Wu[a], Ying Chen[a], Qiang Zheng[a], Wenfang Gu[a]

[a]*Department of Polymer Science and Engineering, Zhejiang University, Zheda Road No. 18, Hangzhou, Zhejiang 310027, China*
[b]*Saint-Gobain Ceramic Materials AS Shanghai, Shanghai 200040, China*

Received 22 October 2004; received in revised form 9 June 2005; accepted 10 June 2005
Available online 15 July 2005

Abstract

We incorporated organic modified layered silicates (OLS) into the mixture of epoxy and poly(ether imide) (PEI) to obtain a ternary hybrid nanocomposite and investigated its reaction-induced phase separation behavior. We found that OLS had dramatic impact to the phase separation process and the final phase morphology. The onset of phase separation and the gelation or vitrification time were greatly brought forward and the periodic distance of phase-separated structure was reduced when OLS was incorporated. Phase separation of the unfilled specimens was greatly suppressed at temperatures higher than 190 °C, and no etch hole of PEI-rich phase could be observed in the SEM images. An interconnected, or bicontinuous morphology could only be observed at cure temperatures lower than 140 °C. On the contrary, the OLS-filled hybrid nanocomposites carried out obvious phase separation at cure temperatures ranging from 120 to 220 °C. Even at cure temperatures higher than 190 °C, the hybrid nanocomposites had an interconnected phase-separated microstructure. These phenomena were related to the preferential wettability, chemical reaction of OLS with epoxy oligomer and the enhanced viscosity of the mixture.

Keywords: Nanocomposites; Montmorillonite; Phase separation

1. Introduction

Both theoretical [1–3] and experimental studies indicates that some fillers particles [4–9] and fibers [10] have important influence to the morphology and phase separation behavior of binary polymer mixtures, especially when the fillers are preferentially wettable to one component of the binary mixtures. For example, glass particles have great impact to the morphology and isothermally-induced phase separation behavior of binary polymer mixtures. The growth rate of SD diminishes when the concentration of filler particles is increased or their diffusivity is decreased. It has been expected that glass particles could be used as a tool to control the morphologies of phase separating binary polymers [4]. Microsized silica particles can lower the phase separation temperature of low molecular weight PS and polybutadiene blends [5]. It was also found that fumed silica changed the phase separation temperatures and kinetics of poly(methyl methacrylate) (PMMA)/poly(vinyl acetate) (PVA) blends [6]. For melting blending immiscible PS/PMMA blends, it was found that oganoclay can drastically reduce the domain size [7]. More recently, Krishnamoorti [8,9] investigated in detail the influence of organoclay to the phase separation behavior of polystyrene/poly(vinyl methyl PS/PVME) blends and found that the phase-separated structure of the nanocomposites has a reduced length scale than that of the unfilled sample. In summary, fillers can greatly affect the phase separation behavior and the final morphology of polymer mixtures. However, to our knowledge, these studies are focused on the isothermally-induced phase separation of binary polymer mixtures but no attentions have been paid to the influence of mobile particles to the reaction induced phase separation behavior and morphology of thermoplastic/thermosetting mixtures up to date.

Phase-separated morphology plays crucial role in

* Corresponding author. Tel.: +86 571 8795 3075; fax: +86 571 87951635.
E-mail address: pengmao@zju.edu.cn (M. Peng).

0032-3861/$ - see front matter © 2005 Elsevier Ltd. All rights reserved.
doi:10.1016/j.polymer.2005.06.013

determining the final properties of these blends [11–26]. The typical example of thermoplastic-thermosetting mixture is the epoxy alloy with modified toughness by blending with high performance thermoplastics, such as poly(ether imide) (PEI), poly(ether sulphone) (PES), poly(phenylene ether) (PPE), polysulphone, poly(ether ketone) (PEK) and so on [11–25]. It has been widely acknowledged that a great increase in toughness is obtained only when the tough thermoplastics form a continuous phase in the mixture. And interpenetrating network with interconnected or bicontinuous phase-separated microstructure, fine domain size and anisotropic phase shape were preferred, because both the toughness of thermoplastics and stiffness of the thermosetting matrix could be combined in the final cured blends. Due to its great importance, study on the controlling of phase-separated morphology has attracted great interests in the last two decades.

The final phase separated morphology of thermoplastics/epoxy mixture is determined by the composition and cure temperature. Thermoplastics/epoxy mixture belongs to a typical dynamically asymmetric mixture [13,26] due to the great differences in molecular weight and glass transition temperatures (T_g) between the two components and its reaction-induced phase separation usually follows the spinodal decomposition (SD) mechanism. The epoxy-rich phase tends to interrupt at even very early stage of SD due to its low viscosity and/or poor fluid strength. The minority phase, namely the thermoplastic-rich phase, is continuous due to its strengthened viscoelasticity during phase separation, but its connectivity is transient. It shrinks gradually and sometimes develops into dispersed spherical droplets with the shape of the lowest interfacial energy at the late stage of phase separation. Usually, higher thermoplastic content is necessary for the formation the co-continuous phase morphology. The phase structure is also controlled by the cure temperature because of the competition between the chemical reaction and physical phase separation. To obtain the interconnected morphology, Inoue [24] suggested lowering the cure temperature toward T_g of the blends or linearly raising the cure temperature gradually, because lower temperature resulted in lowered chain mobility and so reduced phase separation rate. The domain coarsening and interruption of the continuous phase-inversion structure under interfacial tension is also suppressed due to the higher viscosity of the system at lower temperatures. As a result, the co-continuous structure with smaller periodic distance can be fixed when gelation or vitrification occurs earlier than the interruption of continuous domains. However, lowered or programmed cure temperature is usually unacceptable in the industry due to the extremely prolonged cure time and poor efficiency.

On the other hand, polymer/OLS nanocomposites have attracted great interests from both scientists and industrials in the recent years due to their remarkable improvement in mechanical properties, gas barrier properties, flammability resistance [27–38] etc. But as to the toughness, the OLS/epoxy nanocomposites usually have only slightly improved toughness, so Mülhaupt et al combined reactive Liquid rubber with layered silicates to prepare a hybrid epoxy nanocomposites [39]. The toughness of the hybrid nanocomposites is found to be greatly improved compared with the nanocomposites without liquid rubber and has only slightly negative impact to the stiffness. It has been noted that phase-separating structure in the hybrid nanocomposite plays an important role in combination of great toughness and stiffness. However, the phase separation behavior and morphology evolution were not been paid enough attention in their study. And the T_g was lower than that of neat resin by about 30 °C because of the existence of rubber. As high performance thermoplastics have intrinsic high T_g and better mechanical properties than liquid rubbers, hence, one can expect better mechanical properties of thermoplastics hybrid nanocomposites than those based on liquid rubber.

The objective of this study is to investigate the phase separation behavior of thermoplastic/epoxy/OLS ternary hybrid nanocomposites. We believe that the sample used in our study can be a useful model for studying the influence of nanoparticles to the reaction-induced phase separation dynamics. As far as we know, there is no report on this subject in the literature. Compared with the previous studies, the filler particles in our study not only has physically preferential wettablility with epoxy oligomer but also is chemically reactive to epoxy and has complicated intercalation and exfoliation behavior that can interreact with the cure and phase separation processes. In addition, investigations on the viscoelasticity of the organic layered-silicates nanocomposites indicated that incorporation of OLS brought about obviously increased zero-shear viscosity, and it exhibits a solid-like dynamic rheological response at low-frequency region [40–42]. It is reasonable to expect that OLS may bring about obvious influence to the phase separation behavior of thermoplastics-epoxy blends, because viscoelasticity plays a crucial role in the phase separation kinetics and morphology evolution. At the same time, time resolved small angle light scattering (TR-SALS) is a conventional technique in the study of phase separation kinetics of binary polymer mixtures. The influence of OLS to the optical transparency of epoxy resin is quite limited [43]. Therefore, the possibility of using TR-SALS directly to investigate the influence of OLS to the phase separation mechanism and kinetics of hybrid nanocomposites is explored in our study.

2. Experimental

2.1. Materials

The epoxy used in this study is a liquid diglycidyl ether of bisphenol A (DGEBA) type epoxy from Heli Resin Co. Ltd, Suzhou of China, with commercial brand of E51. It has the epoxide equivalent of 194–198 and average molecular

weight of 392 g mol^{-1}. Solvent methylene chloride and curing agent 4,4′-diaminodiphenyl sulfone (DDS) were purchased from the China Medicine (Group) Shanghai Chemical Reagent Corporation, Shanghai, China. PEI employed in this study was GE Ultem® 1000 ($\bar{M}_n = 26,000$ g mol^{-1}, $\bar{M}_w = 50,000$ g mol^{-1}, $T_g =$ 210 °C). Organic modified montmorillonite (MMT) with commercial brand of C18OH-Mt was purchased from the Zhejiang Huate Chemical Co. Ltd, Hangzhou, China. The chemical structure of the cationic surfactant used in C18OH-Mt is presented in Fig. 1. *n* in the molecular formula is from 5 to 8. All above mentioned chemicals and resins were used as received.

2.2. Preparation of samples

Organic modified MMT was dried in vacuum for more than 24 h at 80 °C before experiments. Epoxy oligomer and PEI were weighted and completely dissolved in methylene chloride at room temperature. Then organic modified MMT was dispersed in the solution. The sample was stirred fiercely and then sonicated for at least 20 min. The sample suspensions were translucent but not as clear as solution without OLS. It was interesting that the suspension was rather stable. No precipitations could be observed after being placed at room temperature for several days, indicating that organic modified MMT disperse well in the solution.

The solvent in the solution or suspension was then vaporized in a circulation oven at room temperature until most solvent was removed. Then the samples were placed into a hot vacuum oven preheated to 100 °C to remove the residual solvent in the mixtures. Subsequently, stoichiometric amount of DDS (31.7 phr to epoxy oligomer) was added into the epoxy oligomer/PEI/organic modified MMT mixture and stirred for 5 min in an oil bath at 140 °C until DDS dissolve in the mixture completely. The composition of organic modified MMT, epoxy oligomer, curing agent DDS and PEI for various samples are presented in Table 1. For comparison, the amount of PEI, basing on the sum of epoxy, DDS and PEI, was fixed to 17.5 wt% for the two samples with and without MMT. It should be noted that the amount of PEI in MMT containing mixture was in fact 16.3 wt% in the whole mixture, which is somewhat smaller than that of the unfilled sample.

2.3. Time resolved small angle light scattering (TR-SALS)

Small amount of sample was sandwiched between two

PEI

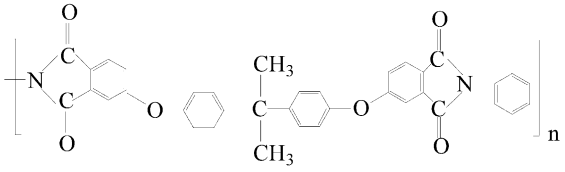

DGEBA

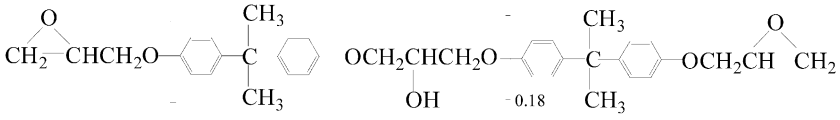

DDS

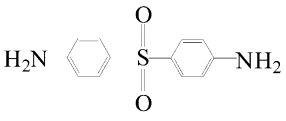

C18OH MMT

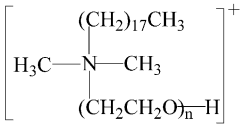

Fig. 1. The chemical structures for DGEBA, DDS, PEI and C18OH.

Table 1
Compositions of the samples used in the study

	Unfilled sample (g)	Filled sample (g)
PEI	1.4	1.4
Epoxy	5.0	5.0
DDS	1.59	1.59
OLS	0	0.6

glass cover slides and pressed into thin film on a hot stage preheated to 90 °C. The unfilled sample films are transparent, while the filled samples are nearly optically clear with only faint blue tint like that usually observed in microemulsions, obviously, this results from the refractive index difference between organic modified MMT and PEI/epoxy matrix.

The laboratory-made time-resolved small angle light scattering apparatus as was used in our proceeding studies [44,45] was employed to investigate the isothermal-curing-induced phase separation behavior of the hybrid nanocomposite in this study. The scattering patterns were recorded by a CCD camera at appropriate time intervals and relationship between scattering intensity and scattering vector were obtained by on-line circular averaging the intensity of the radius symmetric scattering pattern. The integral scattering intensity Q, as is defined in Eq. (1), a parameter reflecting the density inhomogeneity, is also obtained in real time.

$$Q = \int I(q)q^2 \mathrm{d}q = \phi(1-\phi)\Delta n^2 \quad (1)$$

in which, q, $I(q)$, ϕ and Δn are the scattering vector, the scattering intensity at scattering vector q, the volume fraction of one component and the difference in refractive index of the two phases, respectively.

2.4. Scanning electron microscope observation

The samples were placed in a hot oven at 120, 140, 170, 190, 200 and 210 °C, respectively. The cure profile was given in the Table 2. Time for the cure reaction at various temperatures was different. At cure temperatures low than 180 °C, it was difficult for the samples to complete the cure reaction, so the samples were post-cured at 180 °C for another 2 h to ensure a full conversion of the cure reaction. After the cure reaction, the samples were fractured and placed into methylene chloride and stirred fierily for more than 48 h to make sure that the soluble thermoplastic PEI was completely removed. The fractured and rinsed samples were then coated with gold for the SEM observation. The apparatus used in this study was JSM-5510LV from the JEOL Ltd, Japan. All experiments were carried out using a voltage of 20 kV.

Table 2
The cure profiles for the unfilled samples (from (a-1) to (a-6)) and filled samples (from (b-1) to (b-2))

Sample	Cure profiles
a-1	Step 1: 120 °C 48 h; Step 2: 180 °C 2 h
b-1	
a-2	Step 1: 140 °C 12 h; Step 2: 180 °C 2 h
b-2	
a-3	Step 1: 170 °C 4 h; Step 2: 180 °C 2 h
b-3	
a-4	Step 1: 190 °C 3 h
b-4	
a-5	Step 1: 200 °C 2 h
b-5	
a-6	Step 1: 210 °C 2 h
b-6	

2.5. X-ray diffraction (XRD) and thermogrametric analysis (TGA)

Powder X-ray diffraction (XRD) measurements were conducted using a Rigaku D/max 2500 PC diffractometer with a Cu Kα radiation ($\lambda = 0.154$ nm), a tube voltage of 50 kV and a tube current of 40 mA. The scanning speed and the step size were $2^\circ\,\mathrm{min}^{-1}$ and 0.02°, respectively. The range of the 2θ of the scanning X-ray was from 0.5 to 30.0°. The specimens for the XRD measurement were disks with diameter of 2 cm and thickness of 2 mm prepared in a silicone rubber mold.

The residual weight of C18OH-Mt was measured by using a Perkin–Elmer Pyris1 thermogravimetry (TG). To determine whether OLS preferentially distributes in the epoxy-rich or uniformly in the specimen, the average residual weight in the whole specimen was measured and compared with that in the epoxy-rich phase. First, two specimens were cured at 160 °C for 4 h. Then, the residual weight in the unrinsed specimens was measured. Another specimen was sufficiently rinsed in methylene chloride to remove the soluble PEI-rich phase as far as possible. The residual weight in the etched specimen, i.e. in the epoxy-rich phase, was then measured. The measurements were conducted under a dry airflow at a heating rate of 10 °C/min, and the amounts of undecomposed fractions in the products were determined by the residual weight after heating to 900 °C.

3. Results and discussions

3.1. Influence to the morphology

Fig. 2 presents the SEM images of the solvent-etched cross-section of the PEI/epoxy mixture and PEI/epoxy/OLS hybrid nanocomposite after being cured at various temperatures. The shape and size of the PEI-rich phase is thought to be the same to that of the holes.

For the unfilled samples, a co-continuous morphology can be observed at the cure temperatures of 120 °C (a-1) and 140 °C (a-2). Obviously, the holes in images (a-1) and (a-2) has an irregular shape. This structure is commonly observed

during the early and intermediate stage of spinodal decomposition of binary polymer blends.

However, for samples cured at 170 °C (a-3), it is found that large amount of spherical holes can be observed. These holes are apparently isolated, indicating that the PEI-rich phase exists in a form of disrupted spheres in the epoxy-rich matrix. It is interesting that the dispersion of the holes in the matrix is not spatially uniform, on the contrary, some holes line up, indicating that the holes come from the shrinkage and subsequent interruption of the PEI-rich threads at the late stage of phase separation. As a comparison, a SEM image for the unfilled specimen cured at 170 °C for 25 min without post-cure is given in Fig. 3. A co-continuous morphology can be observed, indicating that the phase separation at 170 °C also follows the SD mechanism and the spherical morphology is a result of the interruption of the PEI-rich thread instead of the nucleation-growth (NG) phase separation.

For the samples cured at temperatures higher than 190 °C ((a-4)–(a-6)), the fractured cross-section of the samples were relatively smooth and no etch holes can be observed. So it is believable that phase separation has been suppressed greatly. And as is well known, the smooth fractured cross-section usually results from a brittle impact fracture, indicating the poor toughness of the samples. As was reported in the literature [20,21], the PEI/epoxy mixture has the upper critical solution temperature (UCST) behavior. At phase separation temperatures approaching the cloud point, the composition difference between two phases can be very small. Therefore, the PEI-rich phase cannot be rinsed.

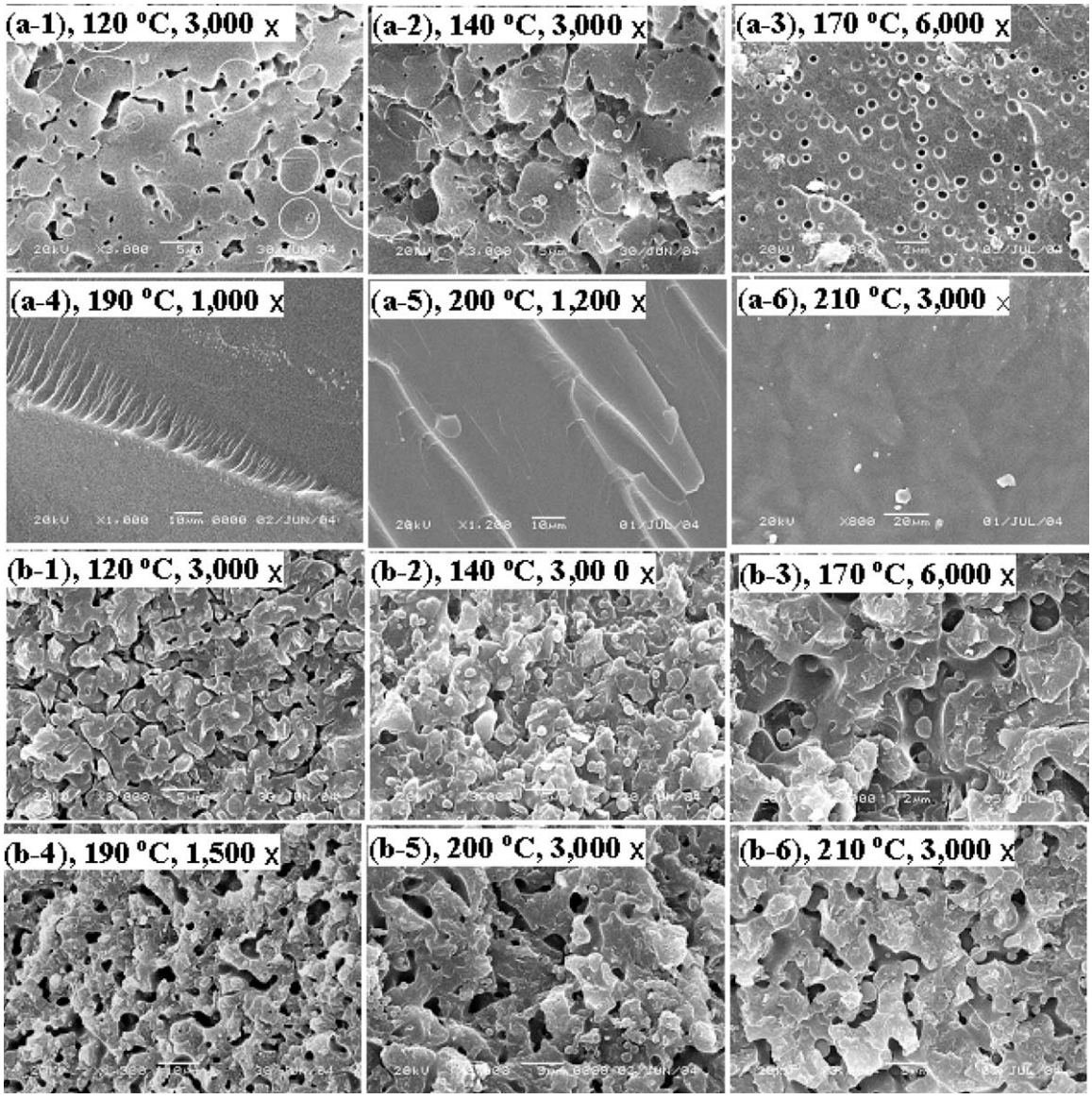

Fig. 2. SEM images for the unfilled PEI/epoxy mixtures (from (a-1) to (a-6)) and those filled with OLS (from (b-1) to (b-6)), after being cured at 120 °C ((a-1), (b-1)); 140 °C ((a-2), (b-2)); 170 °C ((a-3), (b-3)), 190 °C ((a-4), (b-4)); 200 °C ((a-5), (b-5)) and 210 °C ((a-6), (b-6)), respectively. All the samples were rinsed sufficiently by using methylene chloride.

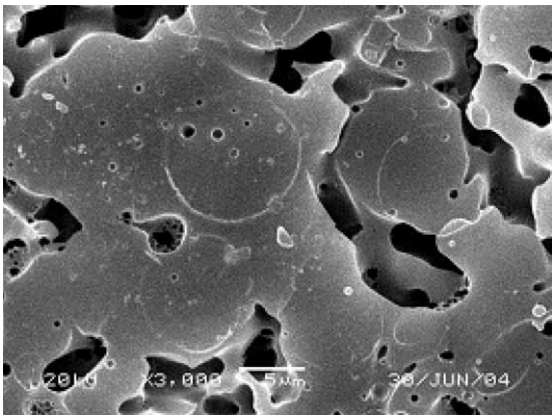

Fig. 3. The SEM image of the PEI/epoxy mixture cured at 170 °C for 25 min.

For the filled specimens from (b-1) to (b-6), the interconnected morphology can be observed for all the samples, regardless of the cure temperature. The etch holes are of irregular shape and connect with each other. This indicates that the phase separation mechanism of the filled samples follows the SD mechanism at all the temperatures.

It should be emphasized that at temperatures higher than 190 °C, the co-continuous structure can still be observed. The difference can also be easily determined through the sample appearance. Filled samples turned to be opaque gradually with the proceeding of the cure reaction at temperatures higher than 190 °C, while the unfilled samples were almost transparent, indicating the optical homogeneity in the samples.

3.2. Influence to the periodic distance

Figs. 4 and 5 give the temporal evolution of scattering patterns and the scattering profiles against scattering vectors for the (a) unfilled and (b) filled specimens at the cure temperature of 170 °C. The definition of scattering vector is $q = (4\pi/\lambda)\sin(\theta/2)$, in which θ and λ are the scattering angle and the wavelength of laser, respectively. It can be found that q_m, the scattering vector with maximum scattering intensity, for the filled specimen is larger than that of the unfilled sample. What should be noted is that the final q_m value for the filled specimen is fixed at 1.22 μm^{-1}, so, the wavelength of composition fluctuation, $\Lambda_m = 2\pi/q_m$, or in other words, the periodic distance of the phase separated structure, is 5.15 μm. As to the unfilled specimen cured at 170 °C, it can be found in Figs. 4(a) and 5(a) that the scattering ring rapidly shrinks. The q_m value at the scattering peak is smaller than 0.5 μm^{-1} before being fixed. This means that the average domain size should be larger than 12.6 μm, but unfortunately, it is too large to be determined correctly by our apparatus. Similarly, the final q_m or Λ_m values for the unfilled specimens cured at 160 and 180 °C also cannot be determined. Fig. 6 gives the periodic distances for the filled and unfilled specimens cured at various temperatures. The solid lines in the figure are used to guide the sights of the readers. It is noted that the Λ_m values for OLS-filled specimens increase from 4.8 to 7.4 μm^{-1} when the cure temperature increase from 120 to 220 °C. These values in fact are in good agreement with what we can observe in the SEM images of Fig. 2(b-1)–(b-6). The periodic distances of unfilled specimens are larger than that of the filled samples when the cure temperature is lower than 180 °C. This indicates that the coarsening of domain size of OLS filled specimens was greatly diminished as the result of OLS incorporation.

Fig. 7 gives the double logarithmic plots of q_m and I_m (maximal scattering intensity) against time for the filled and unfilled specimens cured at 170 °C. Several important features should be noted in this figure. First, one can find that onset of phase separation of filled specimen occurs much earlier than that of unfilled specimen, since q_m and I_m appears much earlier. Then, q_m values of filled specimen decrease in a slower rate than that of unfilled specimen since its absolute value of slope is smaller, as is shown by the triangles in the figure. Thirdly, q_m reaches to its equilibrium much earlier than that of unfilled specimen and the final q_m is much larger than that of the unfilled specimen. Specimens cured at other temperatures also show the same characteristics. This indicates that the coarsening of domain size during phase separation has been greatly diminished after OLS being incorporated, which is in consistence with the theoretical calculation [1] and experimental results [4] basing on the influence of hard particles to the isothermally-induced phase separation behavior of binary polymer blends.

3.3. Time evolution of integral intensity

Fig. 8(a) and (b) presents the temporal evolution of integral scattering intensity Q for the filled and unfilled samples at various isothermal reaction temperatures. The onset time for phase separation, gelation or vitrification and the end of phase separation are denoted by t_{os}, t_{gel} and t_{end}, respectively. For the unfilled specimens, the Q values keep invariant before t_{os}, indicating that no phase separation occurs. But for the filled samples, it is interesting that the Q values slightly increase with time before t_{os}, instead of being invariant. This is related to the influence of OLS. From the scattering profile in Fig. 5(b), one can find that during this stage the scattering light for all the scattering vectors increases gradually and have no scattering peak, indicating that no spatial periodicity in the composition fluctuation. It can be confirmed that OLS have different refractive index with that of the matrix and with the proceeding of curing reaction, the refractive index of the matrix increase with time, this increases the difference of refractive index between OLS and the matrix, and then brings about the increased Q values (Eq. (1)). In the case of the occurrence of phase separation, the scattering light originated from the refractive index differences between the PEI-rich and

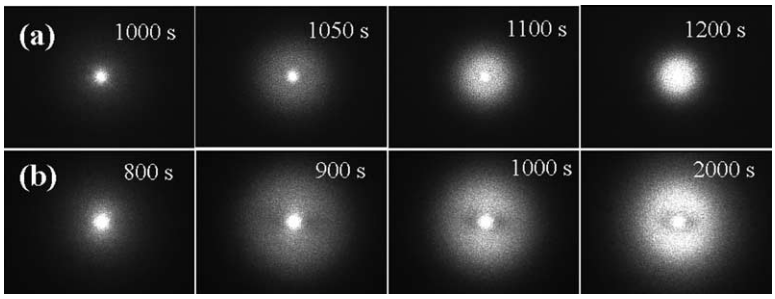

Fig. 4. The temporal evolution of scattering patterns for (a) PEI/epoxy mixture and (b) PEI/epoxy/OLS mixture at the cure temperature of 170 °C.

epoxy-rich phases is so strong that the scattering light related to OLS can be omitted. Therefore, we believe that light scattering is applicable to this hybrid system.

t_{gel} is determined by the time at which the slope for the increase in Q decreases abruptly (Fig. 8) and q_m turns to be invariant in the scattering profiles (Fig. 5(b)). When gelation or vitrification occurs, the mass transport across the boundary between two phases turns to be slower and the evolution of domain size is suppressed. Unfortunately, for the unfilled specimens cured at temperature higher than 160 °C, it is impossible to determine the t_{gel} and t_{end} values, since as mentioned above, the scattering ring decreases is too small to be determined correctly.

Table 3 presents the t_{os}, t_{gel} and t_{end} values for various reaction temperatures. It is noted that these values are greatly brought forward when OLS is incorporated. We define the relative gelation time ($t_{gel,\,r}$) as the ratio of (t_{gel}–t_{os}) against (t_{end}–t_{os}). It should be noted that $t_{gel,\,r}$ for the filled specimens is smaller than that of the unfilled specimens. This indicates that gelation or vitrification occurs at relatively earlier stage, which helps us better understand the mechanism for the formation of interconnected structure in epoxy/PEI/OLS mixture.

Fig. 8(b) presents the time dependence of Q of the filled and unfilled samples at temperatures higher than 190 °C. For the filled samples, the Q values increase sharply even at temperatures as high as 220 °C as the result of apparent phase separation. A notable increase in the Q values for the unfilled PEI/epoxy mixture cured at 190 and 200 °C can also be observed but the maximum Q values are much smaller. This indicates that the composition difference between the two phases is limited. Fig. 9 compares the scattering profiles of filled and unfilled specimens cured at 190 °C. It can be found that for the unfilled specimen, phase separation is greatly suppressed. We observe the same phenomenon for the specimens cured at 200 °C. As to higher cure

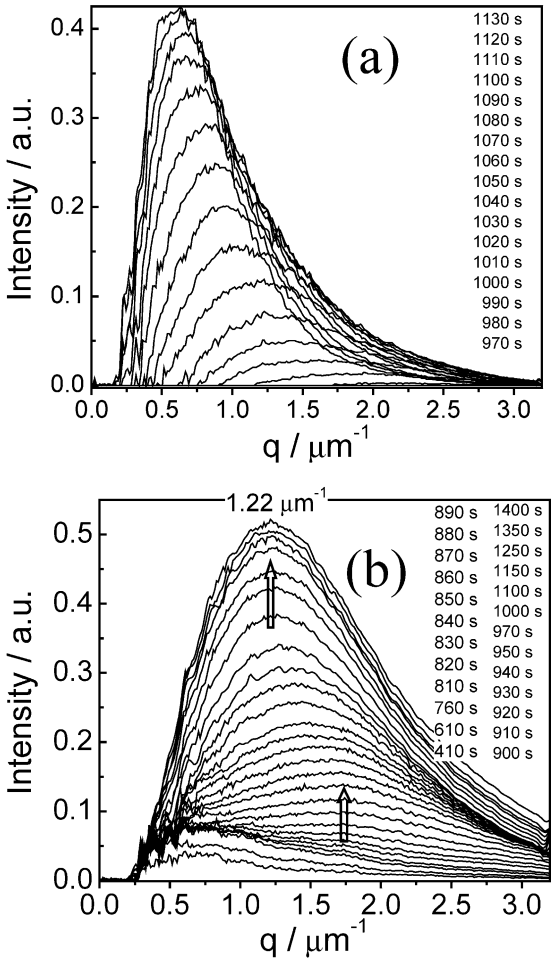

Fig. 5. The temporal evolution of scattering intensity profiles for (a) the PEI/epoxy mixture and (b) the PEI/epoxy/OLS mixture at the cure temperature of 170 °C. The arrows in (b) indicate that the maximum scattering vector keep invariant at the beginning of SD and after the gelation or vitrification.

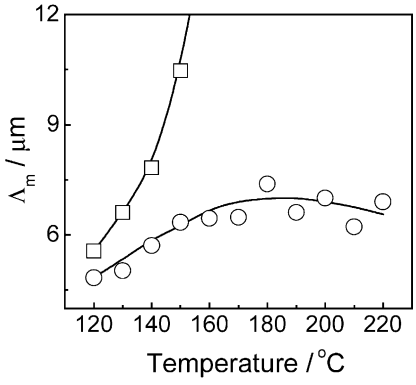

Fig. 6. The temperature dependence of the final periodic distance, Λ_m, for (□) the PEI/epoxy and (○) the PEI/epoxy/OLS mixtures.

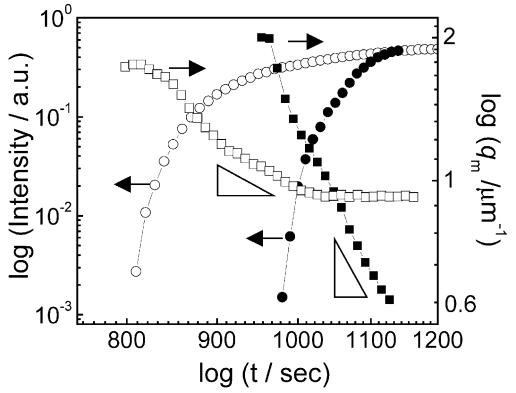

Fig. 7. The double logarithmic plots of time and (■) q_m and (●) I_m for unfilled PEI/epoxy mixture, and (□) q_m and (○) I_m for PEI/epoxy/OLS mixtures. The triangles in the figure show the slopes of the log(q_m)–log(t) plots qualitatively.

temperatures, the Q values keep almost invariant for the unfilled specimens, indicating the complete suppress of phase separation.

As was mentioned above, in the SEM images of (a-4)–(a-6) in Fig. 2, no observable etched holes of the PEI-rich phase can be observed for the unfilled specimens cured at temperatures higher than 190 °C. Whereas, the SALS measurements confirm the occurrence of phase separation at these temperatures. This phenomenon can be interpreted as follows. At cure temperatures approaching the cloud point, phase separation is suppressed and the composition difference between the epoxy-rich and PEI-rich phases is quite limited and the PEI-rich phase cannot be removed by methylene chloride.

Above results indicate that the OLS has greatly increased the phase separation temperature of the PEI/epoxy mixture by about 20 °C. As was mentioned in the experimental section, the total content of PEI in the filled samples is smaller than that of the unfilled ones. Decreasing PEI content usually results in a decrease in cloud point, but it is very interesting that incorporation of OLS to the PEI/epoxy mixture results in a great increase in cloud point.

3.4. XRD and TG measurements

Fig. 10 shows the X-ray diffraction patterns over the range of $2\theta = 0.5 - 10°$ of C18OH-Mt and the PEI/epoxy/OLS mixtures before and after the cure reaction. C18OH-Mt has a strong diffraction peak at $2\theta = 4.5°$, i.e. with an intercalated spacing of $d_{001} = 1.96$ nm. After being mixed with epoxy oligomer, DDS and PEI by solution mixing and drying, the main diffraction peak shifted to $2\theta = 2.38°$, indicating that the intercalated spacing increased to $d_{001} = 3.68$ nm as the result of swelling of C18OH-Mt in the oligomer mixture. The strong diffraction peaks at $2\theta = 4.78°$, $2\theta = 7.12°$ and $2\theta = 9.52°$, corresponding to the interlayer spacing of 1.84, 1.24 and 0.92 nm, respectively. By using the Bragg-law, it can be confirmed that these diffraction peaks correspond to the (002), (003), and (004)

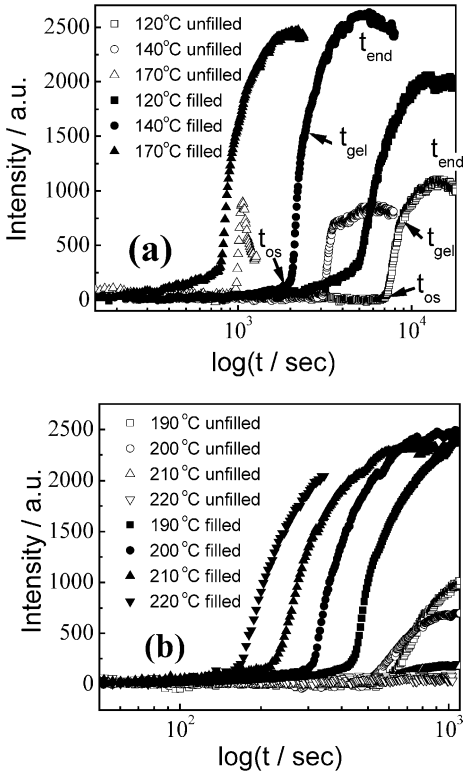

Fig. 8. Evolution of integral scattering intensity Q at cure temperatures of (a) 120, 140, 170 °C, and (b) 190, 200, 210 and 220 °C, respectively, for filled and unfilled PEI/epoxy mixtures.

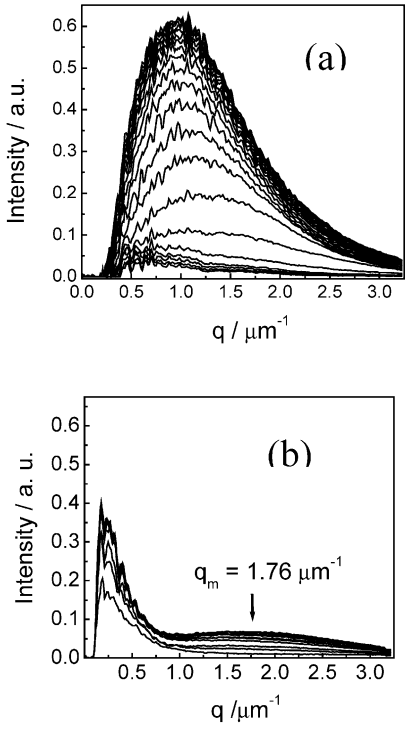

Fig. 9. Comparison of the temporal evolution of scattering profiles for (a) the filled specimen and (b) the unfilled specimen at the cure temperature of 190 °C.

Table 3
The time for the onset of phase separation, the gelation or vitrification, the end of phase separation and the relative gelation time for the filled and unfilled specimens

T (°C)	Epoxy/PEI				Epoxy/PEI/OLS			
	t_{os} (s)	t_{gl} (s)	t_{end} (s)	$t_{gel,\ r}$	t_{os} (s)	t_{gl} (s)	t_{end} (s)	$t_{gel,r}$
120	7150	8670	13,780	0.229	4967	6340	12,130	0.192
130	4728	5605	8902	0.210	3518	4200	7180	0.186
140	3035	3600	5750	0.208	2043	2428	4050	0.192
150	2066	2420	3749	0.210	1413	1780	3420	0.183
160	1344	–	–	–	1060	1330	2541	0.182
170	979	–	–	–	770	915	1625	0.170
180	731	–	–	–	568	730	1550	0.165
190	560	–	–	–	437	548	1156	0.154
200	494	–	–	–	310	390	820	0.157
210	–	–	–	–	220	286	645	0.155
220	–	–	–	–	168	200	372	0.157

planes of C18OH-Mt in the matrix. This indicates that the intercalated and stacked structure of OLS in the matrix of oligomer mixture is very regular. More important, there is a small diffraction peak at $2\theta = 0.82°$, which corresponds to the interlayer spacing of 10.7 nm. This indicates that part of OLS in the oligomer mixture has a nearly exfoliated structure before the cure reaction. In Fig. 10(c), it can be found that the main diffraction peak is at $d_{001} = 3.80$ nm, which is only slightly larger than that before curing, indicating that the intercalated spacing has been slightly enlarged. Furthermore, it should also be noted that the height of the main diffraction peak turned to be lower and the width of the peak, i.e. the width at the half-maximum of the peak, turned to be much wider than that before curing. There also appeared a shoulder-peak at the left side of the main diffraction peak with the $2\theta = 1.42°$ and the spacing of 6.2 nm. This indicates that more epoxy molecules intercalate into the intergallery region of OLS, resulting in the further swelling of OLS during the cure reaction. At the same time, in comparison with the XRD pattern in Fig. 10(b), the diffraction peak at 10.7 nm in the uncured specimen disappeared after cure reaction. A reasonable explanation to this phenomenon is that this peak shift to lower diffraction angle that cannot be detected because of the complete exfoliation of this part of OLS in the matrix during the cure reaction. As was reported in the literature [46–48], OLS in DGEBA could be completely exfoliated when using DDS as the curing agent. Our study indicate that high molecular polymer like PEI has negative impact to the exfoliation behavior of OLS in the epoxy matrix. But it can be concluded that after curing, the OLS in the epoxy/PEI hybrid nanocomposite have a mainly intercalated structure accompanied by a partly exfoliated structure.

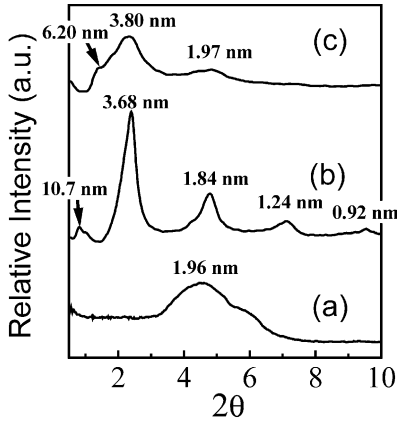

Fig. 10. The XRD diffraction patterns for (a) organic modified MMT C18OH-Mt; (b) PEI/epoxy/OLS mixture before curing reaction and (c) the PEI/epoxy/OLS mixture after being cured at 170 °C for 4 h.

Results of TG measurements were given in Fig. 11. The residual weight in the C18OH-Mt is 68.9% by weight. The residual weight in the unetched specimen is 4.52 wt%, which is close to 4.80 wt%, the theoretically calculated residual weight according to the concentration of OLS in the whole mixture. What should be noted is that the residual weight in the epoxy-rich region, namely, in the sufficiently etched specimen, is 5.40 wt%, which is much higher than the average residual weight in the whole mixture. Basing on this fact, one can conclude that OLS is preferentially wettable to epoxy oligomer and/or its curing agent. During the reaction-induced phase separation, OLS gradually concentrate in the epoxy-rich region.

3.5. Mechanism for the interconnected morphology

The final morphology of reaction-induced phase-separation mixture is fixed when gelation or vitrification occurs. The phase separation structure is usually interconnected when it is fixed at the early stage or the intermediate stage. Here, we consider the mechanism for the formation of interconnected structure observed in the filled specimens cured at relatively high temperatures.

Park [48], Simon [49] and some other authors investigated the influence of OLS to the cure reaction of DGEBA type epoxy, and found that the cure reaction rate was increased because of the catalytic effect of protonated alkylammonium cation in the OLS to the cure reaction of

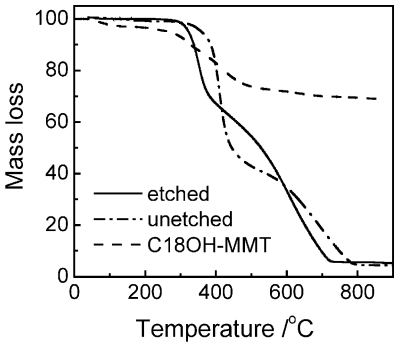

Fig. 11. The TGA cures for C18OH-Mt, not-rinsed specimen of PEI/epoxy/OLS mixture and sufficiently rinsed specimen of PEI/epoxy/OLS mixture in methylene dichloride.

epoxy. This can interpret the earlier onset of phase separation and gelation time for filled specimens. However, the relaxation of I_m and q_m slows down, indicating that phase separation rate is obviously decreased for the filled mixture. Hence, the phase structure at the early or the intermediate stage of phase separation can be more easily fixed.

We believe that the delayed relaxation rate of SD is related to the increased viscosity of the system. Many authors [40,42,43] have investigated the influence of OLS on the viscoelasticity behavior of the OLS based nanocomposites for various polymer matrixes. It has been found that the zero shear viscosity of the OLS containing polymer increase with the increase of clay content and is related with the structure of OLS dispersing in the matrix. OLS can be intercalated, partially or completely exfoliated in the polymer matrix. Not only for samples with completely exfoliated OLS but also for those with only intercalated or partially exfoliated OLS, the viscosity can be increased greatly. Increase in zero shear viscosity by several times, and in some cases by one or even more order of magnitudes can be observed. And non-Newtonian fluid behavior, such as the strong shear thinning or a solid-like yielding behavior can also be observed in these materials. The strong interaction between epoxy molecules and the surface of silicate platelets resulting from the chemical reaction and physical adhesion, and the geometric confinement effect of inorganic fillers to the mobility of molecules are crucial to the increased viscosity. In our experiment, the specimen has intercalated and partially exfoliated structure, and the OLS particles concentrate in the epoxy-rich region, therefore, it is reasonable to believe that the viscosity of the epoxy-rich region is increased obviously compared with that of neat resin.

In the early stage of SD, an exchange of mass occurs across the boundary of the two phases, and molecules diffuse from lower concentration region to higher concentration region, therefore, the phase separation is strongly controlled by the mass transport efficiency of the system. The relationship between the time evolution of concentration and the mobility coefficient can be described by using the well-known Cahn–Hilliard equation for SD kinetics, as follows:

$$\frac{\partial \phi}{\partial t} = M\left[\left(\frac{\partial^2 f}{\partial \phi^2}\right)\nabla^2\phi - 2\kappa\nabla^4\phi\right]$$

where M, ϕ, κ and f are the mobility coefficient, the volume fraction of one component, the gradient energy coefficient, and the free energy of mixing, respectively. The definition of mobility coefficient M of an uncharged solid single sphere with the radius of a in the well-known Einstein–Stokes equation is defined as $M=6\pi\eta a$, where η is the fluid medium viscosity. Although this definition is limited to a single sphere in an unbounded fluid and the practice system is much more complicated, the fact that M is direct proportional to the medium viscosity indicates that the relaxation time of SD increases with the medium viscosity at the early stage of SD.

At the late stage of phase separation, the coarsening of domain size is mainly determined by the viscosity and interface tension and follows Siggia's equation: $dR/dt \propto \delta/\eta$ in which R is the diameter of the domain size, η is the viscosity, δ is the interface tension [50]. The increase in viscosity brings about the delayed coarsening of the domain size. At the same time, the shape relaxation time from a thin thread to a sphere and can be characterized by a time of $\eta R/\delta$ [26]. Hence, the increases in viscosity enlarge the shape relaxation time for the OLS containing composites, namely the co-continuous phase structure at early stage of phase separation can be more easily fixed. Therefore, an increased viscosity facilitates the formation of co-continuous structure by influencing both the early and late stage of phase separation.

3.6. Influence to the cloud point

Lipatov [6] found that fumed silica increased the cloud points of PMMA/PVA by about 10 °C, resulting from the change of interactions among the components. In our study, the phase separation temperature of PEI/epoxy mixture is increased by more than 20 °C. As far as we know, no other filler particles like OLS having such strong effect to the miscibility and cloud point have been reported before. This phenomenon may be qualitatively explained by the possible influence of C18OH modified MMT to the interaction and miscibility between PEI and epoxy. But we believe that the intercalation or exfoliation behavior of OLS during the cure reaction should also be taken into consideration. As was observed in the TG measurement, OLS particles were preferentially included in the epoxy-rich region. This phenomenon was not only resulted from the physically preferential wetability of OLS to epoxy but also resulted from the chemical reaction of protonated alkylammonium cation with epoxy oligomer and the diffusion of molecules into the intergallery region of the C18OH modified MMT. PEI is a polymer with slower diffusivity than that of epoxy

oligomer and does not react with C18OH, therefore, it is reasonable to speculate that the epoxy oligomer selectively diffuse into the intergallery region of OLS, i.e. more epoxy oligomer molecules than PEI molecules diffuse into the intergallery of OLS, bringing about the increase in PEI concentration in the extragallery region and so the increased cloud point of the whole mixture. This speculation can be at least partially supported by the SEM images of PEI/epoxy/OLS mixtures in Fig. 2 and those with larger magnification presented in Fig. 12, in which one can observe a large amount of interconnected small epoxy-spheres with diameter of about 1–2 μm in the etched holes, namely, the PEI-rich region. Similar nodular structure can be hardly observed in samples without OLS in our experiments and can usually be observed in PEI/epoxy mixture with higher PEI concentration [51].

4. Conclusion remarks

We investigated the influence of OLS to the reaction-induced phase separation behavior of thermoplastic/epoxy mixture by using SALS and SEM over a wide cure temperature range. Although the transparency of OLS containing samples was not as good as that of binary polymer blends, the results indicated that light scattering of OLS is quite limited and the SALS was appropriate to the study of phase separation behavior of OLS filled nanocomposites. SD mechanism was observed in the hybrid nanocomposites. More important, it was found that OLS greatly affected the phase separation behavior both thermodynamically and kinetically. Apparent SD for samples filled with OLS could be observed at temperatures much higher than the phase separation temperature of unfilled specimens. The coarsening of SD was also obviously diminished, resulting in phase-separated structure with fine periodic distances. At the same time, the final morphology of the hybrid nanocomposite was interconnected at the cure temperature even higher than 190 °C, in contrast with the fact that the unfilled PEI/epoxy mixtures having interconnected phase morphology only at the cure temperatures lower than 140 °C. In the viewpoint of applications, our study can broaden the potential applications of OLS. In comparison with the previous studies, incorporation of OLS is a novel, facile and effective method to create thermoplastics/epoxy blends with an interconnected morphology and modified toughness at relatively high cure temperatures.

Acknowledgements

We are appreciated to the financial support from the National Natural Science Foundation of China (Grant No.50203013).

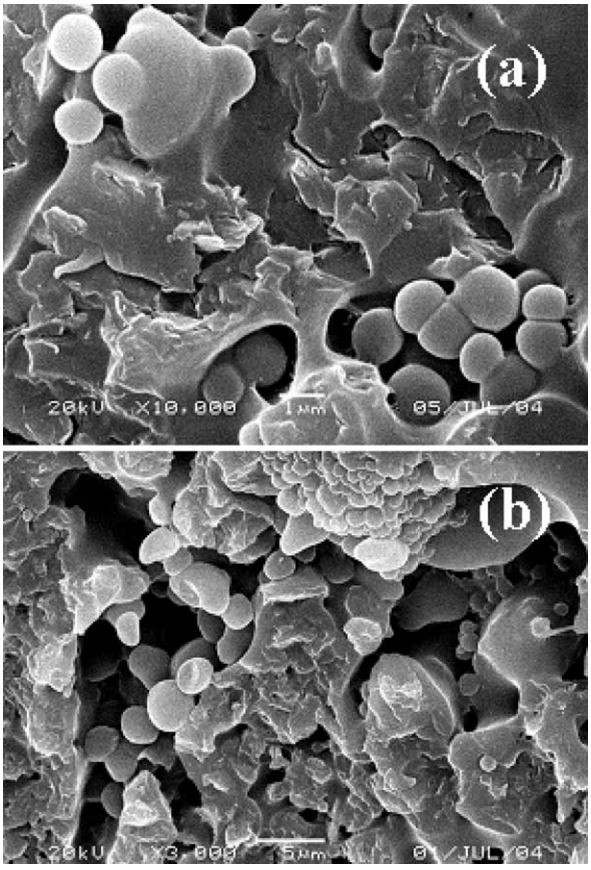

Fig. 12. SEM images of the connected-globular structure in the PEI-rich phase for PEI/epoxy/OLS mixture at the cure temperatures of (a)160 °C and (b) 180 °C, respectively.

References

[1] Ginzburg VV, Qiu F, Paniconi M, Peng GW, Jasnow D, Balazs AC. Phys Rev Lett 1999;20:4026–9.
[2] Laradjia M. J Chem Phys 2004;19:9330–5.
[3] Zhu YJ, Ma YQ. Phys Rev E 2003;67:041503.
[4] Tanaka H. Phys Rev Lett 1994;16:2581–4.
[5] Karim A, Liu D-W, douglas JF, Nakatani AI, Amis EJ. Polymer 2000; 41:8455.
[6] Nesterov AE, Lipatov YS, Horichko VV, Iganatova T. Macromol Chem Phys 1998;199:2609–12.
[7] Gelfer MY, Song HH, Liu L, Hsiao BS, Chu B, Rafailovich M, et al. Polym Sci, Part B: Polym Phys 2003;41:44–54.
[8] Yurekli K, Karim A, Amis EJ, Krishnamoorti R. Macromoecules 2003;36:7256–67.
[9] Yurekli K, Karim A, Amis EJ, Krishnamoorti R. Macromoecules 2004;37:507–15.
[10] Turmel DJ-P, Partidge IK. Compos Sci Technol 1997;57:1001–7.
[11] Wang Z, Wang H, Shimizu K, Dong JY, Hsiao BS, Han CC, Polymer, 2005;8:2675–84.
[12] Lestriez B, Chapel JP, Gérard JF. Macromolecules 2001;34:1204–13.
[13] Gan W, Yu Y, Wang M, Tao Q, Li S. Macromolecules 2003;20: 7746–51.
[14] Bonnet A, Pascault JP, Sautereau H, Rogozinski J, Kranbuehl D. Macromolecules 2000;10:3833–43.
[15] Bonnet A, Pascault JP, Sautereau H, Camberlin Y. Macromolecules 1999;25:8524–30.
[16] Pethrick RA, Hollins EA, McEwan I, MacKinnon AJ, Hayward D, Cannon LA, et al. Macromolecules 1996;29(15):5208–14.

[17] Wang M, Yu YF, Wu XG, Li S. Polymer 2004;45:1253–9.
[18] Su CC, Woo EM. Polymer 1995;15:2883–94.
[19] Yu Y, Zhang Z, Gan W, Wang M, Li S. Ind Eng Chem Res 2003;14: 3250–6.
[20] Mimura K, Ito H, Fujioka H. Polymer 2000;41:4451–9.
[21] Kim BS, Chiba T, Inoue T. Polymer 1995;36(1):43–7.
[22] Girard-Reydet E, Sautereau H, Pascault JP, Keates P, Navard P, Thollet G, et al. Polymer 1998;39(11):2269–80.
[23] Xie X, Yang H. Mater Des 2001;22:7–9.
[24] Mimura K, Ito H, Fujioka H. Polymer 2000;41:4451–9.
[25] Inoue T. Prog Polym Sci 1995;20:119–53.
[26] Tanaka H. Phys Rev Lett 1996;76(5):787–90.
[27] Kojima Y, Usuki A, Kawasumi M, Okada A, Fukushima Y, Kurauchi T, et al. Mater Res 1993;8:1185–9.
[28] Yano K, Usuki A, Okada A. J Polym Sci, Part A: Polym Chem 1997; 35:2289–94.
[29] Gilman JW, Kashiwagi T, Lichtenhan JD. SAMPE J 1997;33:40–6.
[30] Vaia RA, Price G, Ruth PN, Nguyen HT, Lichtenhan JD. Appl Clay Sci 1999;15:67–92.
[31] Yoshihiro S, Mitsuhiro S. Polymer 2005;46(13/17):4891–8.
[32] Maged AO, Jörg EPR, Ulrich WS. Polymer 2005;46(5/14):1653–60.
[33] Yei DR, Kuo SW, Fu HK, Chang FC. Polymer 2005;46(3/26):741–50.
[34] Choi YS, Xu M, Chung IJ. Polymer 2005;46(2/12):531–8.
[35] Zhang Z, Zhang L, Li Y, Xu H. Polymer 2005;46(1/6):129–36.
[36] Yalcin B, Cakmak M. Polymer 2004;45(19/3):6623–38.
[37] Leslie Sl, Karen KG. Polymer 2004;45(17/5):5933–9.
[38] Yei DR, Kuo SW, Su YC, Chang FC. Polymer 2004;45(8):2633–40.
[39] Fröhlich J, Thomann R, Mülhaupt R. Macromolecules 2003;36: 7205–11.
[40] Lee KM, Han CD. Macromolecules 2003;36:7165–78.
[41] Galgali G, Ramesh C, Lele A. Macromolecules 2001;34:852–8.
[42] Maiti P. Langmuir 2003;19:5502–10.
[43] Brown JM, Curliss D, Vaia RA. Chem Mater 2000;12:3376–84.
[44] Zheng Q, Peng M, Song YH, Zhao TJ. Macromolecules 2001;34: 8483.
[45] Peng M, Yuan XX. Macromol Chem Phys 2004;205:256–65.
[46] Park J, Jana SC. Macromolecules 2003;36:8391–7.
[47] Wang Z, Pinnavaia TJ. Chem Mater 1998;10:1820–6.
[48] Kong D, Park CE. Chem Mater 2003;15:419–24.
[49] Becker O, Cheng Y-B, Varley RJ, Simon GP. Macromolecules 2003; 36(5):1616–25.
[50] Siggia ED. Phys Rev A 1979;20:595.
[51] Park JW, Kim SC. Polym Adv Technol 1995;7:209–20.